NATIONAL ADVISORY COMMITTEE FOR AERONAUTICS

REPORT No. 536

WIND-TUNNEL TESTS OF A 10-FOOT-DIAMETER GYROPLANE ROTOR

By JOHN B. WHEATLEY and CARLTON BIOLETTI

1935

For sale by the Superintendent of Documents, Washington, D. C. - - - - - - - - - - - - - - Price 5 cents

AERONAUTIC SYMBOLS

1. FUNDAMENTAL AND DERIVED UNITS

	Symbol	Metric		English	
		Unit	Abbreviation	Unit	Abbreviation
Length	l	meter	m	foot (or mile)	ft. (or mi.)
Time	t	second	s	second (or hour)	sec. (or hr.)
Force	F	weight of 1 kilogram	kg	weight of 1 pound	lb.
Power	l'	horsepower (metric)		horsepower	hp.
Speed	V	kilometers per hour	k.p.h.	miles per hour	m.p.h.
		meters per second	m.p.s.	feet per second	f.p.s.

2. GENERAL SYMBOLS

W, Weight $= mg$

g, Standard acceleration of gravity $= 9.80665$ m/s^2 or 32.1740 ft./sec.^{2}

m, Mass $= \frac{W}{g}$

I, Moment of inertia $= mk^2$. (Indicate axis of radius of gyration k by proper subscript.)

μ, Coefficient of viscosity

ν, Kinematic viscosity

ρ, Density (mass per unit volume)

Standard density of dry air, 0.12497 kg-m^{-4}-s^2 at 15° C. and 760 mm; or 0.002378 lb.-ft.$^{-4}$ sec.^{2}

Specific weight of "standard" air, 1.2255 kg/m^3 or 0.07651 lb./cu.ft.

3. AERODYNAMIC SYMBOLS

S, Area

S_w, Area of wing

G, Gap

b, Span

c, Chord

$\frac{b^2}{S}$, Aspect ratio

V, True air speed

q, Dynamic pressure $= \frac{1}{2}\rho V^2$

L, Lift, absolute coefficient $C_L = \frac{L}{qS}$

D, Drag, absolute coefficient $C_D = \frac{D}{qS}$

D_o, Profile drag, absolute coefficient $C_{D_o} = \frac{D_o}{qS}$

D_i, Induced drag, absolute coefficient $C_{D_i} = \frac{D_i}{qS}$

D_p, Parasite drag, absolute coefficient $C_{D_p} = \frac{D_p}{qS}$

C, Cross-wind force, absolute coefficient $C_C = \frac{C}{qS}$

R, Resultant force

i_w, Angle of setting of wings (relative to thrust line)

i_t, Angle of stabilizer setting (relative to thrust line)

Q, Resultant moment

Ω, Resultant angular velocity

$\rho\frac{Vl}{\mu}$, Reynolds Number, where l is a linear dimension (e.g., for a model airfoil 3 in. chord, 100 m.p.h. normal pressure at 15° C., the corresponding number is 234,000; or for a model of 10 cm chord, 40 m.p.s. the corresponding number is 274,000)

C_p, Center-of-pressure coefficient (ratio of distance of $c.p.$ from leading edge to chord length)

α, Angle of attack

ϵ, Angle of downwash

α_o, Angle of attack, infinite aspect ratio

α_i, Angle of attack, induced

α_a, Angle of attack, absolute (measured from zero-lift position)

γ, Flight-path angle

REPORT No. 536

WIND-TUNNEL TESTS OF A 10-FOOT-DIAMETER GYROPLANE ROTOR

By JOHN B. WHEATLEY and CARLTON BIOLETTI
Langley Memorial Aeronautical Laboratory

394—35——1

NATIONAL ADVISORY COMMITTEE FOR AERONAUTICS

HEADQUARTERS, NAVY BUILDING, WASHINGTON, D. C.

LABORATORIES, LANGLEY FIELD, VA.

Created by act of Congress approved March 3, 1915, for the supervision and direction of the scientific study of the problems of flight. Its membership was increased to 15 by act approved March 2, 1929. The members are appointed by the President, and serve as such without compensation.

TECHNICAL COMMITTEES

AERODYNAMICS
POWER PLANTS FOR AIRCRAFT
AIRCRAFT STRUCTURES AND MATERIALS

AIRCRAFT ACCIDENTS
INVENTIONS AND DESIGNS

Coordination of Research Needs of Military and Civil Aviation

Preparation of Research Programs

Allocation of Problems

Prevention of Duplication

Consideration of Inventions

LANGLEY MEMORIAL AERONAUTICAL LABORATORY

LANGLEY FIELD, VA.

Unified conduct, for all agencies, of scientific research on the fundamental problems of flight.

OFFICE OF AERONAUTICAL INTELLIGENCE

WASHINGTON, D. C.

Collection, classification, compilation, and dissemination of scientific and technical information on aeronautics.

REPORT No. 536

WIND-TUNNEL TESTS OF A 10-FOOT-DIAMETER GYROPLANE ROTOR

By John B. Wheatley and Carlton Bioletti

SUMMARY

This paper presents the results of wind-tunnel tests on a model gyroplane rotor 10 feet in diameter. The rotor blades had zero sweepback and zero offset; the hub contained a feathering mechanism that provided control of the rotor rolling moment, but not of the pitching moment. The rotor was tested with 4 blades and with 2 blades. The entire useful range of pitch settings and tip-speed ratios was investigated including the phase of operation in which the rotor turned very slowly, or idled.

The results afford valuable information concerning the influences of pitch setting, solidity, and feathering angle upon the rotor characteristics. The feathering control appeared to be satisfactory in the normal flying range but showed a marked decrease in effectiveness at very low tip-speed ratios. A feathering angle considerably greater than the 10° that was provided was required at high tip-speed ratios and high pitch settings to obtain zero rolling moment. Unfortunately, because the rotor hub was disproportionately large, the measured lift-drag ratios are considered to be inexact.

INTRODUCTION

The National Advisory Committee for Aeronautics has for several years been studying different types of rotating-wing systems because of their pronounced advantages in respect to safe flight. These advantages are derived mainly from the fact that the air speed of the lifting surfaces of the rotating wing is almost independent of the forward speed of the machine so that large air forces are, under all conditions, available for lift and control.

One of the systems studied was the gyroplane, which is of the autorotating type. Opposite blades of the rotor are rigidly connected and the thrusts on each side of the plane of symmetry are equalized by an oscillation, or feathering, of the blade pair about an axis approximately parallel to the span axis. The oscillation can be automatic if the blade center of thrust is behind the feathering axis; a controlled feathering, effected by a cam arrangement in the hub, is usually employed which generates rolling or pitching moments as desired so that conventional elevators and ailerons are unnecessary.

An aerodymic ananalysis of the gyroplane (reference 1) indicated that experimental studies of the system were warranted. Previous experimental investigations of the gyroplane rotor have consisted entirely of low-scale wind-tunnel tests. Several full-scale machines have been built and flown but no published information concerning these efforts is available. The model tests reported in this paper were consequently planned to give results at a large scale and to obtain complete information on the effect of as many as possible of the design variables of the rotor. The model was 10 feet in diameter and was operated at full-scale tip speed; provisions were made for the study of changes in the blade oscillation, blade pitch angle, and the solidity.

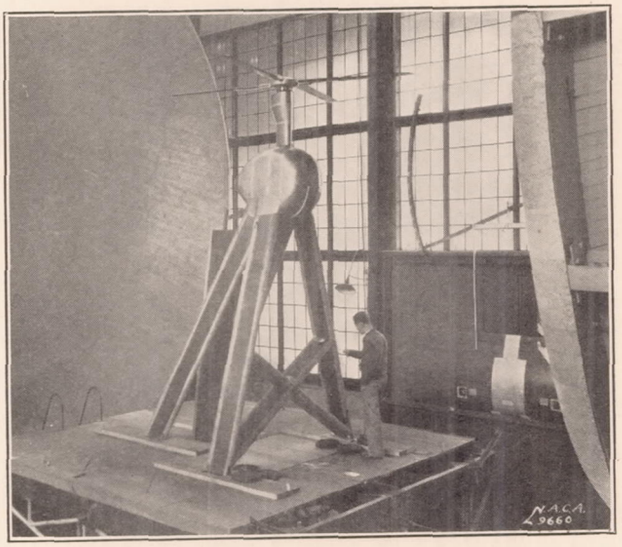

FIGURE 1.—Ten-foot-diameter gyroplane rotor mounted for test.

APPARATUS

The tests were performed in the N. A. C. A. 20-foot wind tunnel described in reference 2. The balance system was as therein described except for the addition of two lateral-force balances. The model mounted for testing is shown in figure 1.

The rotor was 10.04 feet in diameter and consisted of four blades having constant chords of 6.28 inches and semielliptical tips. The blades were constructed of laminated mahogany; the airfoil section used

was the N. A. C. A. 0015. Each pair of blades was mounted on the ends of a steel shaft, the butts of the blades being bolted to forks forged in the ends of the shaft. The pitch of the blades could be varied from 0° to 6° in 1° steps by wedges inserted between the forks and the blade butts. Bearings in the hub permitted each blade pair to oscillate (or feather) about its span axis through the quarter-chord points of the blade sections. The axes of the two blades of the pair and the feathering axis were coincident.

A mechanism was provided for feathering the blade pairs as the rotor revolved. This mechanism is shown schematically in figure 2. When the control is set for zero feathering, the instantaneous pitch of all the blades is equal to the pitch setting a_0 throughout the entire revolution. When feathering is introduced, the pitch of the advancing blade is decreased and of the retreating blade increased, the deflection being a

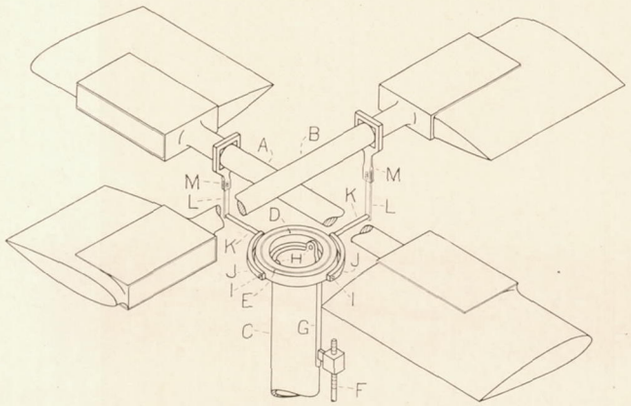

FIGURE 2.—Schematic diagram of blade-feathering mechanism for gyroplane rotor.

maximum when the pair of blades is in the cross-wind position and zero when in the fore-and-aft position.

The shafts A and B are supported in bearings mounted on a hub (not shown in fig. 2). The tube C does not turn with the rotor but provides a support for D, which is the inner race of a ball bearing. The outer race E revolves with the rotor. The control shaft F can be turned by means of a hand crank, thereby raising rod G that is connected to D. This motion tilts the ball bearing about the pivots H. The two pins I extend into E and the arms J rotate the outer race E of the bearing. A sleeve (not shown in the figure) supports the two shafts K in bearings. The sleeve also supports the hub and, in turn, the shafts A and B. When the bearing D–E is tilted, the pins I rise and fall with respect to the shafts K as the rotor turns. The shafts K being held in bearings, an oscillation is imparted to arms L and, in turn, to the arms M that oscillate the shafts A and B. The motion of the blades differs very slightly from simple harmonic motion because of a small change in the effective length of the arms L as the deflection changes. By means of this feathering of the blades the rolling moment could be controlled but, as the bearing D–E could only be tilted about one axis, control of pitching moments could not be obtained.

The tube C, which also carried the bearings of the rotor hub (not shown in fig. 2), was held in a frame attached to an electric motor, the whole being mounted on trunnion bearings so that the angle of attack of the rotor could be varied from 0° to 90°. A sting and tailpost were used to control the angle of attack. The rotor was mounted inverted, that is, the lift was directed downward. The angle of attack was increased by inclining the rotor axis upstream, thus bringing the rotor ahead of the supports and their shielding and reducing their interference effect on the rotor. As shown in figure 1, all of the supporting structure except the sting, part of the tailpost, and the streamlined mast supporting the rotor were shielded.

The electric motor used for starting the rotor was a 220-volt alternating-current induction motor capable of delivering about 4 horsepower at 550 revolutions per minute. It was connected to the rotor through an overrunning clutch by a shaft; the motor friction was smaller than that in the clutch, however, so the motor usually turned with the rotor. The motor had ball bearings and the friction added to the rotor during the tests was small.

TESTS AND PROCEDURE

The rotor was tested with four blades at pitch settings of 0°, 1°, 2°, 3°, 4°, 5°, and 6°. One pair of blades and the connecting shaft were then removed and the resultant two-bladed rotor was tested at 0°, 2°, 4°, and 6°. Each pitch setting was tested at tip-speed ratios from 0 to 0.8, except that the 0° and 6° pitch settings of the two-bladed rotor were not tested below a value of about 0.1; at 0°, the lowest tunnel speed resulted in a dangerously high rotor speed, and at 6° autorotation broke down in that range. Additional tests were made on both rotors at angles of attack of from 0° to 5°, resulting in tip-speed ratios of from 4.0 to 1.5. This condition is called "idling."

Tare lift and tare drag were determined with the entire rotor and hub removed from the streamlined mast, which was left exposed to the air stream. In an effort to determine the drag due to the hub and the forks that held the blades, tests were made with the hub in place and with short wooden stubs of the same form as the butts of the blades held in the forks. The hub and stub blades were rotated at 550 revolutions per minute during the test by means of the starting motor. This test was performed also with one pair of forks and stub blades removed. The tare runs were made at several air speeds and, as the scale effect was rather large, the values of tare C_L and tare C_D at each angle of attack were taken at the speed corresponding to the air speed during the test of the rotor at that angle of attack.

A few trials were made to discover whether or not the rotor would start by itself if exposed to the air stream. There appeared to be a critical angle of attack below which the rotor was self-starting and above which the rotor tended to turn in the reverse direction. This critical angle of attack varied with the pitch setting, being about 20° for a pitch setting of 0° and about 8° for a pitch setting of 6°. After the rotor had started, the angle of attack could be increased above the critical value previously mentioned and the speed would increase unless the angle of attack were increased too rapidly when the rotor was still turning slowly. In this case the rotor would slow down, stop, and start in the reverse direction.

An attempt was made to estimate the extent of the effect of blocking the tunnel when the rotor was at a high angle of attack. The force on the rotor at 90° angle of attack is of the same order of magnitude as the force on a disk of the same diameter normal to the air stream. Accordingly, a disk 10 feet in diameter was tested normal to the air stream at low speed, and a disk 2.25 feet in diameter was also tested at a speed giving the same Reynolds Number.

At the beginning of each test the rotor was brought up to speed by the electric starting motor and the tunnel fan was then started. The starting motor was then switched off and the model was allowed to autorotate. When the air speed had become steady, the angle of attack and the feathering angle were set and recorded; when the rotor speed became constant, simultaneous visual observations of dynamic pressure, rotor speed, and balance scale readings were taken. Throughout the tests, readings were taken at each tip-speed ratio with the estimated feathering angle for zero rolling moment and with 1° larger and 1° smaller feathering angle. Preliminary tests at a moderate air speed were made to permit an estimate of the feathering angle required. In this manner the rolling moment was kept small and in most cases both positive and negative rolling moments were obtained.

The rotor was operated at 550 revolutions per minute, which resulted in a tip speed of 288 feet per second; this value is approximately the same as that of a full-scale rotor. In the range of angles of attack between 30° and 90°, the rotor speed at a given pitch setting was not influenced appreciably by angle of attack; the tunnel speed was accordingly held constant over this range. The tunnel speed resulting in a rotor speed of 550 revolutions per minute in the high-angle-of-attack range varied with different pitch settings from 34 feet per second for 0° pitch setting to 50 feet per second for 6°. The low-angle-of-attack range was tested by increasing the tunnel speed above the values previously given and adjusting the angle of attack to maintain a rotor speed of 550 revolutions per minute. In the tests of the four-bladed rotor when the tunnel speed reached 125 feet per second, it was kept constant and additional readings were obtained by reducing the angle of attack, which resulted in lower rotor speeds; the lowest rotor speed obtained in this condition was about 300 revolutions per minute. The readings obtained at a constant air speed of 125 feet per second corresponded to tip-speed ratios of from 0.43 to 0.80. During the tests of the two-bladed rotor, the range of tip-speed ratios from 0.43 to 0.80 was obtained by using a constant rotor speed of 305 revolutions per minute and varying the tunnel speed from 70 feet per second to 125 feet per second.

394—35——2

RESULTS

The terminology and symbols used in this paper are identical with those employed in reference 1. Positive axes for the rotor in its normal position are: X, forward; Y, toward advancing blade (toward right); and Z, downward. Moments are positive in cyclic order; that is, moment about the X axis is positive if it moves the positive Y into the positive Z axis, etc. The origin is at the intersection of the rotor axis with the plane of the rotor disk. For convenience, a list of symbols, definitions, and units is appended.

V, True air speed, ft./sec.

Ω, Rotor angular velocity, rad./sec.

R, Rotor radius, ft.

α, Angle of attack, deg. (acute angle between relative wind and plane perpendicular to rotor axis).

L, Rotor lift, lb.

D, Rotor drag, lb.

T, Rotor thrust, lb. (component of rotor force parallel to rotor axis).

Y, Rotor lateral force, lb.

L', Rotor rolling moment, lb.-ft.

M, Rotor pitching moment, lb.-ft.

a_0, Rotor blade pitch setting, deg.

b_1, Feathering angle, deg.

C_L, Lift coefficient, $\frac{L}{\frac{1}{2}\rho V^2\pi R^2}$

C_D, Drag coefficient, $\frac{D}{\frac{1}{2}\rho V^2\pi R^2}$

C_R, Resultant-force coefficient $(C_L^2+C_D^2)^{\frac{1}{2}}$

C_T, Thrust coefficient, $\frac{T}{\rho\Omega^2\pi R^4}$

C_Y, Lateral-force coefficient, $\frac{Y}{\frac{1}{2}\rho V^2\pi R^2}$

C_l, Rolling-moment coefficient, $\frac{L'}{\frac{1}{2}\rho V^2\pi R^3}$

C_m, Pitching-moment coefficient, $\frac{M}{\frac{1}{2}\rho V^2\pi R^3}$

μ, Tip-speed ratio, $\frac{V\cos\alpha}{\Omega R}$

ψ, Blade azimuth angle from down wind in direction of rotation.

The feathering angle b_1 is the coefficient of sin ψ in the series that expresses the instantaneous pitch angle θ of the rotor blade. (See reference 1.)

$$\theta = a_0 - a_1 \cos \psi - b_1 \sin \psi - a_3 \cos 3\psi - b_3 \sin 3\psi$$

In the foregoing series, a_0 is the blade pitch setting. The model was so constructed for these tests that all the terms in the series except a_0 and b_1 were zero.

The test procedure was such that at each pitch setting a large number of test points were obtained that followed a more or less systematic variation with tip-speed ratio and rolling moment. The experimental coefficients were then cross-faired to obtain the values corresponding to zero rolling moment and were then plotted against tip-speed ratio. It was impossible to extrapolate some of the test points to this condition because the variation of rolling moment was unsystematic at low tip-speed ratios ($\mu < 0.1$); in addition, at high tip-speed ratios ($\mu > 0.7$) the required feathering

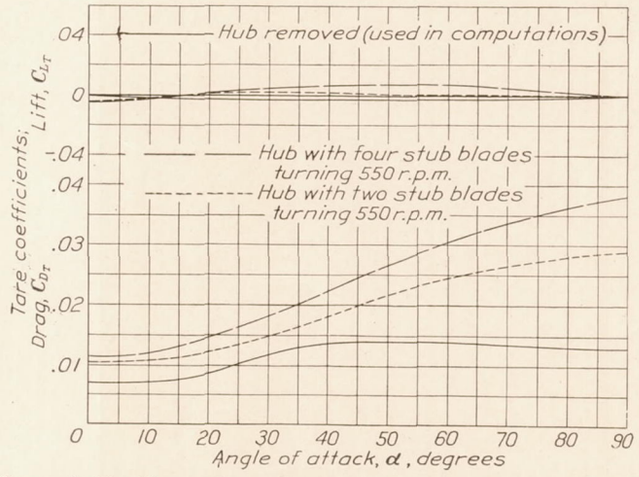

FIGURE 3.—Tare lift and drag coefficients based on disk area of 10-foot-diameter gyroplane rotor, with hub removed, and with 2 and 4 stub blades turning 550 revolutions per minute.

angle was greater than the maximum obtainable with the model. In these cases, which occurred at very low and at very high tip-speed ratios, the average of the test points was used without regard to the value of the rolling moment. The resultant curves were then cross-faired against pitch setting so that accidental variations in the test results could be minimized.

The net forces used in computing coefficients were obtained in all cases by deducting from the measured forces the forces developed during tare tests with the rotor blades and hub removed. The justification of the use of this tare value is more completely covered in the discussion. The different tares obtained are shown in figure 3.

Complete results for the four-bladed rotor at 0°, 1°, 2°, 3°, 4°, 5°, and 6° pitch settings are given in figures 4 to 13, inclusive. Curves are presented showing the lift coefficient, lift-drag ratio, resultant-force coefficient, thrust coefficient, angle of attack, feathering angle for zero rolling moment, slope of the rolling-moment-coefficient curve with feathering angle, lateral-force coefficient, and pitching-moment coefficient as functions of the tip-speed ratio for each pitch setting tested. The lateral-force, pitching-moment, and idling coefficients are, however, given only for 0°, 2°, 4°, and 6° pitch settings. Idling lift and drag coefficients are plotted against angle of attack in figure 13. The same quantities are presented, in order, for the two-bladed rotor at pitch settings of 0°, 2°, 4°, and 6° in figures 14 to 23. The lift-drag ratio is given in preference to the drag coefficient because the drag coefficient varied between such wide limits that an unwieldly scale would have been required to plot it; the lift-drag ratio is just as useful and is more easily presented.

ACCURACY

The accidental errors in the test results arose from such sources as fluctuations in the rotor speed, failure to synchronize all observations, the presence of vibrations in the model, and uncertainty regarding the value of the feathering angle because of play in the mechanical linkage. The influence of such errors is minimized by the large number of test points and the careful cross-fairing of all data.

There are two important sources of consistent errors. One is the blocking effect, which is important only above 30° angle of attack; the second is the tare drag, which influences the results appreciably only at angles of attack below 30°. The influence of these factors upon the results cannot be quantitatively evaluated; their bearing upon the results is considered at length in the discussion.

The following table represents the probable magnitude of the errors in the faired curves of various quantities due solely to accidental sources:

For $\mu > 0.2$		For $\mu < 0.2$	
C_L	±3%	C_L	±4%
L/D	±5%	C_R	±3%
C_T	±4%	C_T	±4%
C_Y	±0.001	C_Y	±0.003
C_m	±0.005	C_m	±0.010
α	±0.25°	α	±0.25°
b_1	±0.25°	b_1	±0.25°
a_0	±0.1°	a_0	±0.1°

DISCUSSION

Tare drag.—The differences obtained from tare tests with the hub removed and with the hub and forks in place are illustrated in figure 3. At low angles of attack the differences are 60 percent of the net drag for low pitch settings. The tare coefficients used to compute the net coefficients were those obtained with the hub removed; if the tare obtained with the hub, forks, and stub blades in place were used, the net results would correspond approximately to the coefficients of a rotor in which the inner 25 percent of the radius was imaginary. In addition, a full-scale rotor

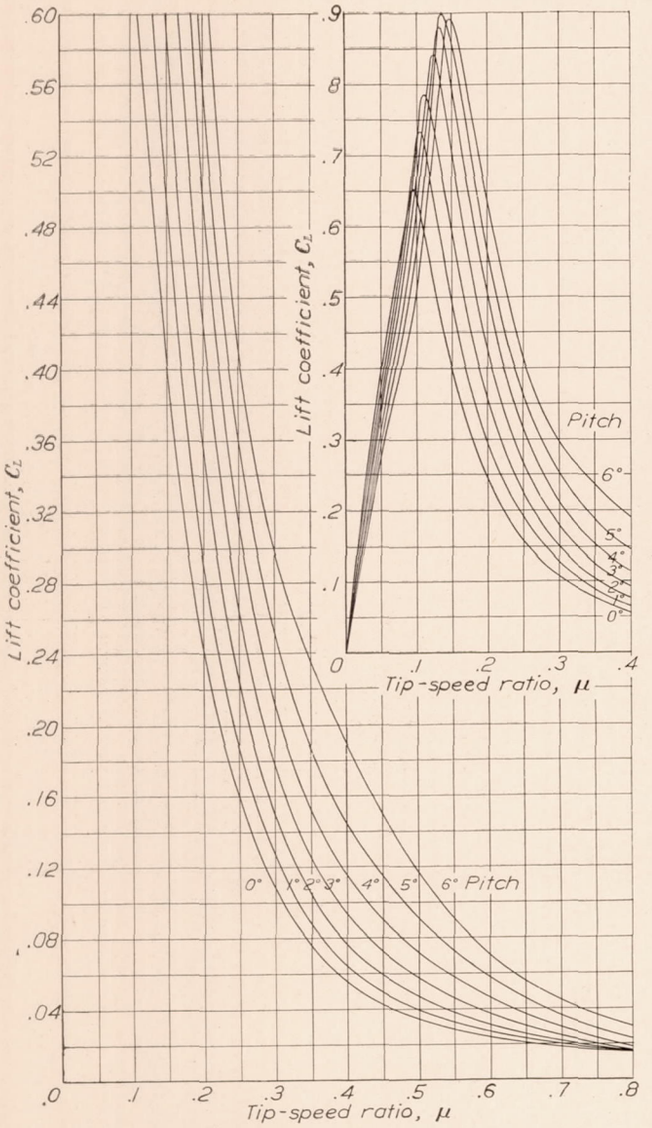

FIGURE 4.—Lift coefficient C_L of 10-foot gyroplane rotor, four blades.

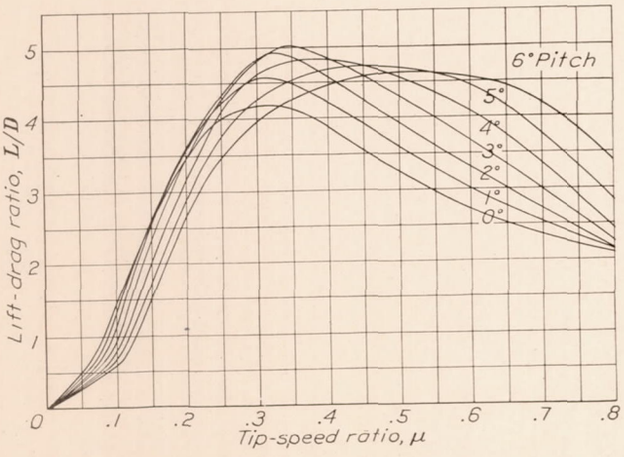

FIGURE 5.—Lift-drag ratio L/D of 10-foot gyroplane rotor, four blades.

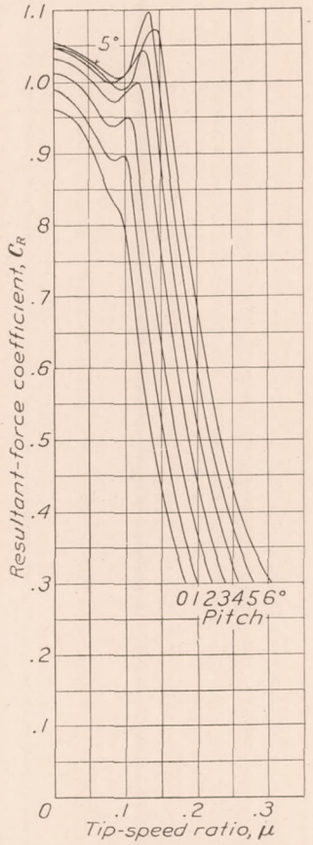

FIGURE 6.—Resultant-force coefficient C_R of 10-foot gyroplane rotor, four blades.

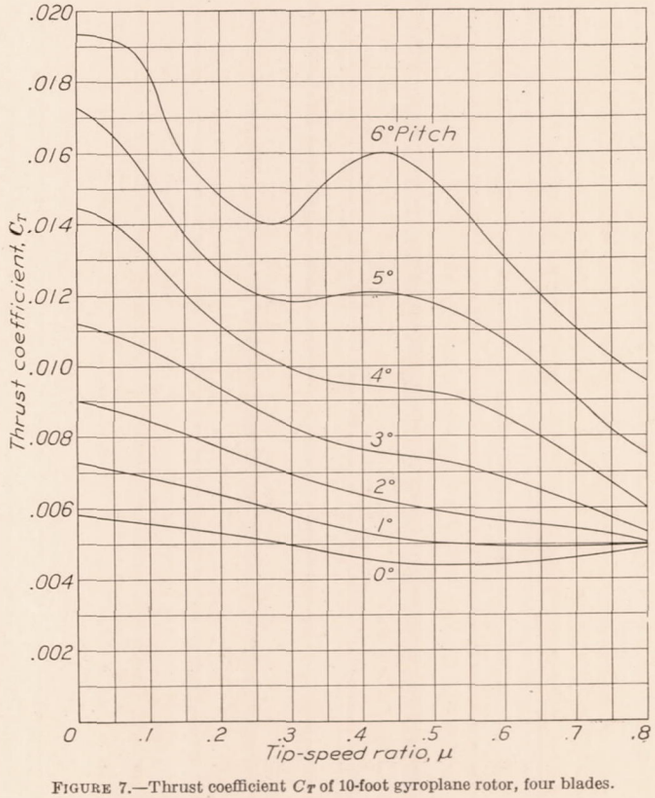

FIGURE 7.—Thrust coefficient C_T of 10-foot gyroplane rotor, four blades.

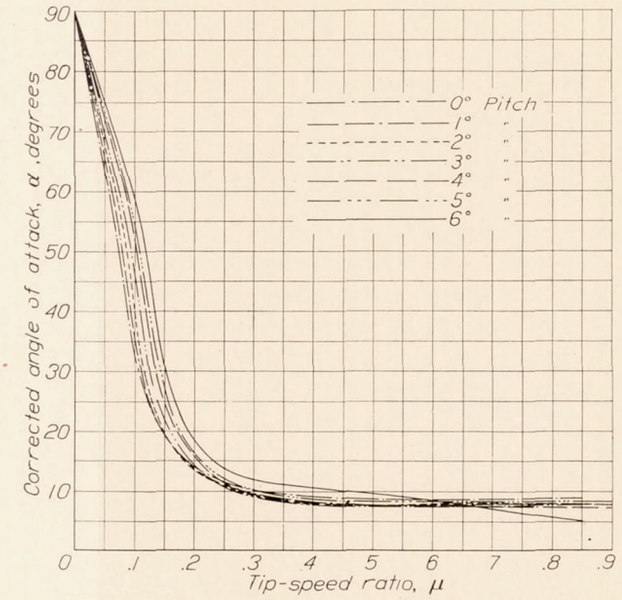

FIGURE 8.—Rotor angle of attack α as a function of tip-speed ratio, 10-foot gyroplane rotor, four blades.

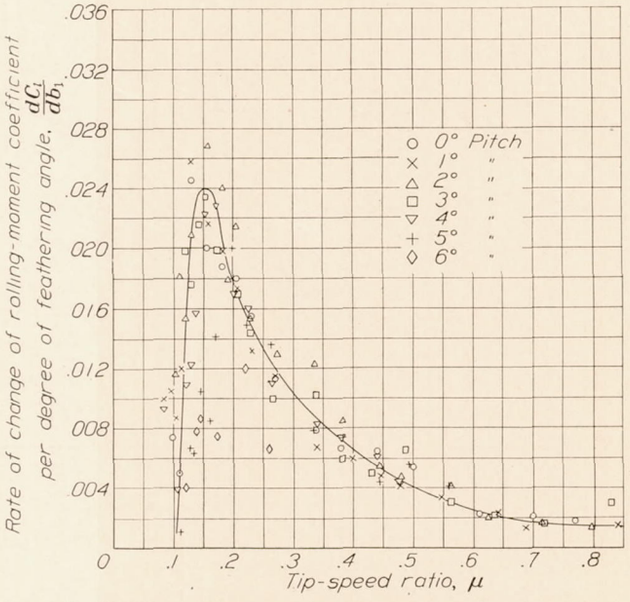

FIGURE 10.—Variation with tip-speed ratio of slope of rolling-moment coefficient against feathering angle dC_l/db_1 for 10-foot gyroplane rotor, four blades.

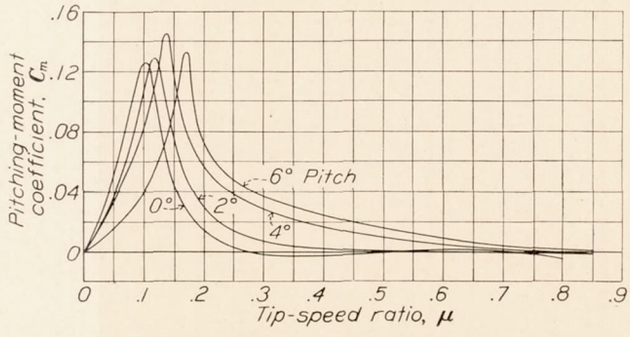

FIGURE 12.—Pitching-moment coefficient C_m of 10-foot gyroplane rotor, four blades.

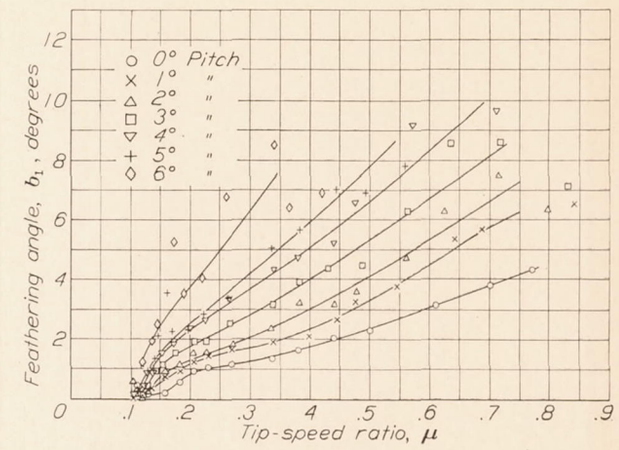

FIGURE 9.—Feathering angle b_1 for zero rolling moment, 10-foot gyroplane rotor four blades.

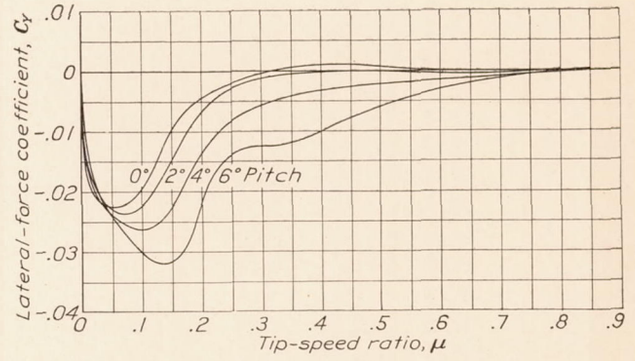

FIGURE 11.—Lateral-force coefficient C_Y of 10-foot gyroplane rotor, four blades.

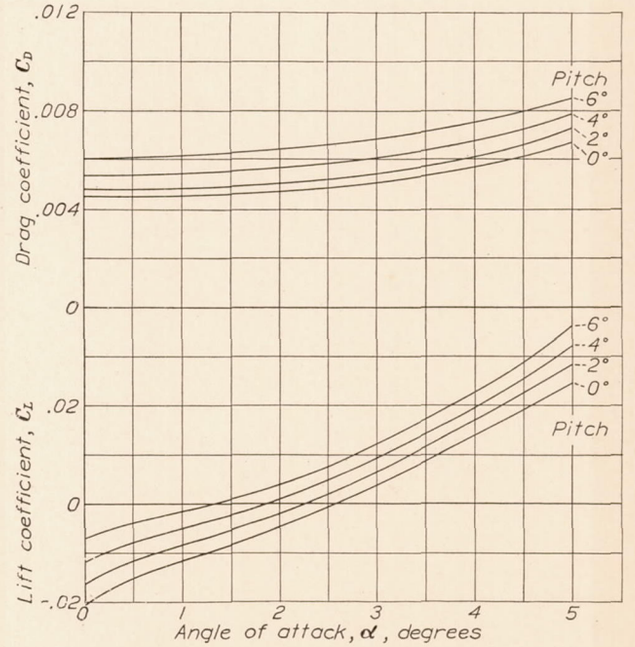

FIGURE 13.—Lift coefficient C_L and drag coefficient C_D with rotor idling, zer feathering, 10-foot gyroplane rotor, four blades.

must have a hub that will be, in general, similar to the model hub, although slightly smaller proportionally and perhaps better streamlined. It was accordingly decided that the employment of the tare obtained with the entire hub removed would give results corresponding more closely to an actual full-scale rotor than could be obtained by the use of any of the other tares obtained. It is to be expected, however, that a full-scale rotor will develop slightly higher values of the lift-drag ratio than the model because of the possibility of reducing the hub drag.

Jet-boundary and blocking corrections.—Jet-boundary corrections were applied to the test results by assuming that the correction was the same as that for an airfoil of the same span and total lift. Fortunately, the correction was very small when the rotor operated at high tip-speed ratios in the range of the maximum lift-drag ratio so that values in that range are unaffected by any error in the assumption. There is undoubtedly an error, because the rotor obviously has a trailing vortex field different from that of a wing; information on this subject is completely lacking, however, so that the assumption made was the only one possible. Even at low tip-speed ratios it is thought that the error in the jet-boundary correction is a very small percentage of the net drag and at high tip-speed ratios the correction vanishes. The influence of the jet boundary upon the net test results is consequently thought to be negligible.

An attempt to evaluate the effect of blocking upon the rotor was made by testing two disks of different sizes at the same Reynolds Number. The disks were 2.25 and 10 feet in diameter and, when normal to the air stream, developed drag coefficients of 1.307 and 0.972, respectively. The drag of the 10-foot-diameter disk was of the same order of magnitude as the drag of the rotor. If the velocity field near the 10-foot disk were similar to that near the rotor, the disk test would indicate that the measured rotor-drag coefficients at 90° angle of attack should be multiplied by $\frac{1.307}{0.972}$ to obtain free-air values; the differences between the disk and rotor, however, preclude such an operation. Since the blocking effect results in an erroneously low measured drag coefficient and is approximately proportional to the drag coefficient, the relative positions of the rotor-drag coefficients at different pitch settings are not changed by blocking. The measured rotor coefficients at high angles of attack should consequently be increased, but not all by the same amount, to give free-air values. Blocking effect can be neglected at angles of attack below about 30° so the coefficients of the rotor in the range of maximum lift-drag ratio are unaffected by it. No correction was applied to the test data to remove the blocking effect because of the uncertainty regarding its magnitude in the range where the effect was appreciable.

Pitch setting.—The pitch setting a_0 of the rotor blade is a major factor influencing the values of C_L (fig. 4, 14), L/D (figs. 5, 15), C_T (figs. 7, 17), and b_1 for zero rolling moment (figs. 9, 19). At a given tip-speed ratio in the normal flying range, an increase in a_0 increases C_L, C_T, and b_1. The influence of a_0 on L/D is interesting, since the tip-speed ratio at which the L/D is a maximum depends upon a_0; as a_0 increases, μ for $(L/D)_{max}$ increases. The highest L/D obtained was developed when the pitch setting was 30; but a change in the tare drag would have a more pronounced influence on the low- than on the high-pitch settings because of the lower coefficients obtained at low-pitch settings and would probably alter the pitch setting for $(L/D)_{max}$.

Feathering angle b_1.—The feathering angles b_1 for zero rolling moment shown in figures 9 and 19 are incomplete for pitch settings higher than 4° because the maximum obtainable feathering angle, 10°, was too small to obtain zero or positive rolling moments at high-pitch settings. The progressive change in the required b_1 at a given μ as a_0 increases is clearly shown in the figures. The points shown in figures 9 and 19 are not test points but represent values obtained from the intersection of an experimental curve with the axis of zero rolling moment.

The rate of change of rolling-moment coefficient with feathering angle when the rolling moment is zero is shown in figures 10 and 20. As the data showed no consistent variation of $\frac{dC_l}{db_1}$ with pitch setting, the one curve drawn in each figure applies to all pitches. The variation in $\frac{dC_l}{db_1}$ with tip-speed ratio is such that $\frac{dC_l}{db_1}$ is small when μ is large and increases as μ decreases until a limit of $\mu = 0.15$ is reached. Since a decrease in μ requires a decrease in velocity, the increase in $\frac{dC_l}{db_1}$ will tend to neutralize the decrease in dynamic pressure and approximately the same feathering angle will be required to develop a given rolling moment at either end of the normal speed range. There is a danger, however, in the pronounced decrease of $\frac{dC_l}{db_1}$ when μ becomes less than 0.15; this effect indicates that at very low speeds the controls would tend to "soften" and excessive control movements would result in relatively small control moments.

Pitching moments were generated by the model because no provision was made to rotate the controllable bearing race (D, fig. 2) about the longitudinal axis. These moments are shown in coefficient form in figures 12 and 22; they are thought to be of secondary interest because they can be controlled, as the rolling moment was, by so constructing the control mechanism that the bearing race D could be rotated about the desired axis.

Resultant force.—The measured resultant-force coefficients of the rotor at each pitch setting tested are

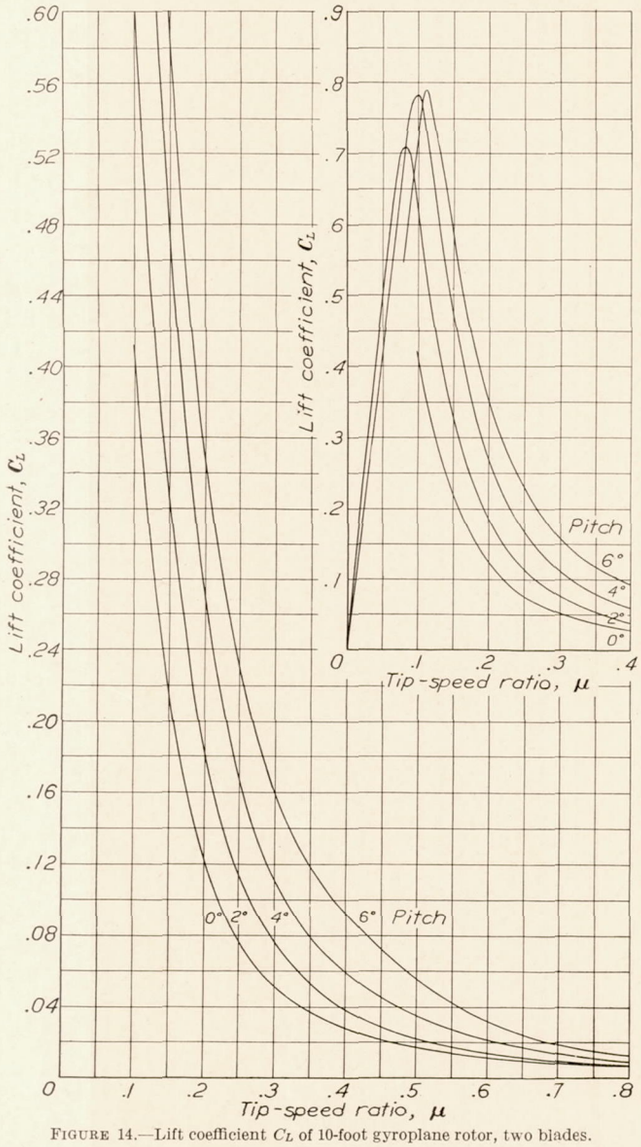

FIGURE 14.—Lift coefficient C_L of 10-foot gyroplane rotor, two blades.

shown in figures 6 and 16. The irregularities in the curves at low values of μ can be qualitatively explained

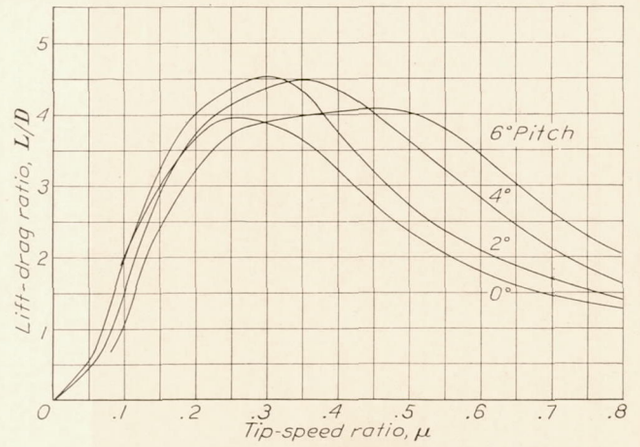

FIGURE 15.—Lift-drag ratio L/D of 10-foot gyroplane rotor, two blades.

as an influence of the blocking effect, which would be appreciable only at high angles of attack and at large drag coefficients. The maximum normal-force coefficient was developed at a pitch setting of 5°.

Thrust coefficient.—The test data on thrust coefficients are shown in figures 7 and 17. The influence of pitch setting is clearly demonstrated and appears to be quite consistent. Irregularities, which appear to be

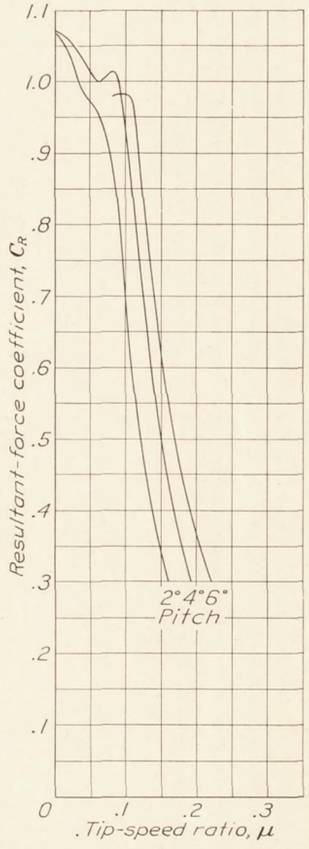

FIGURE 16.—Resultant-force coefficient C_R of 10-foot gyroplane rotor, two blades.

caused by a stalling of the blade elements, appear in the thrust coefficients at low values of the tip-speed ratio and at high pitch settings. This explanation is supported by observations noted during the tests, when peculiar sounds were heard at high pitch settings and high angles of attack, indicating unsteady air flow; in addition, difficulties were encountered in main-

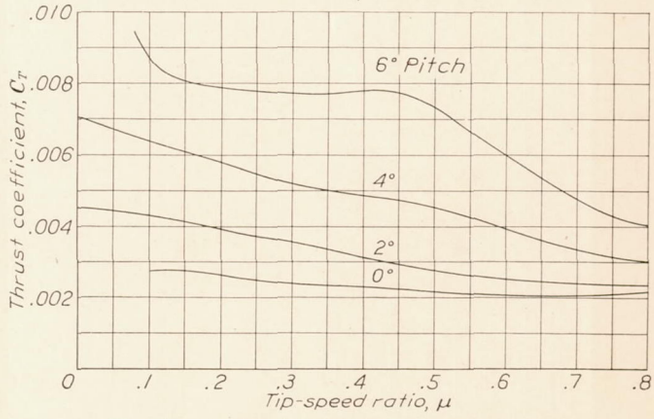

FIGURE 17.—Thrust coefficient C_T of 10-foot gyroplane rotor, two blades.

taining autorotation in the range mentioned and the rotation seemed less stable.

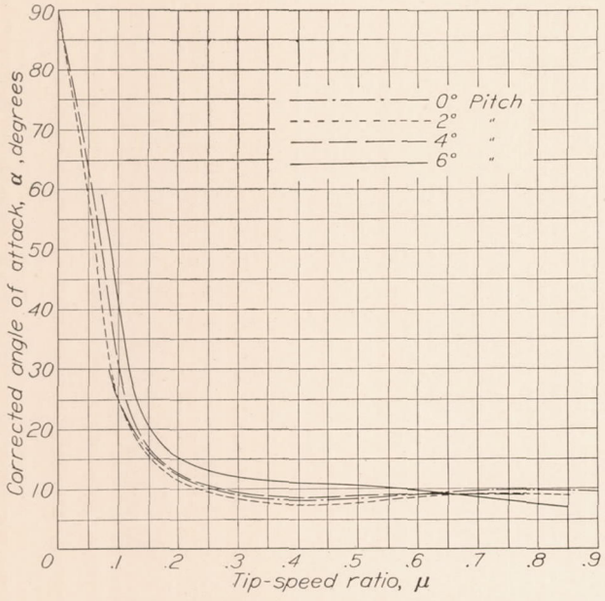

FIGURE 18.—Rotor angle of attack α as a function of tip-speed ratio, 10-foot gyroplane rotor, two blades.

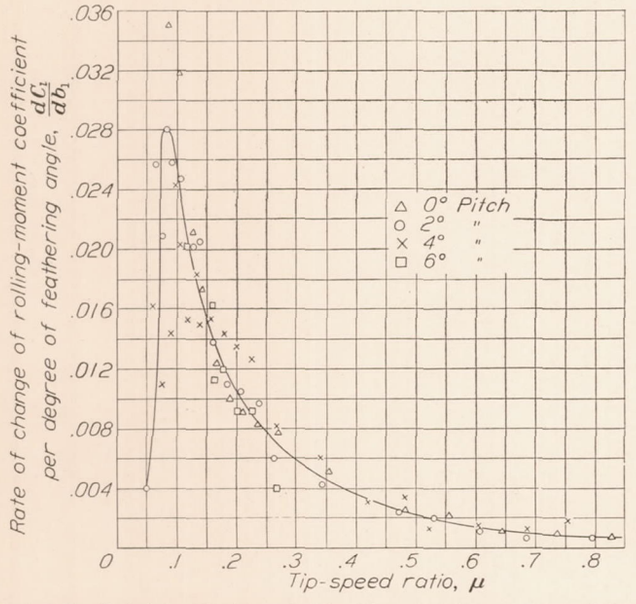

FIGURE 20.—Variation with tip-speed ratio of slope of rolling-moment coefficient against feathering angle dC_l/db_1 for 10-foot gyroplane rotor, two blades.

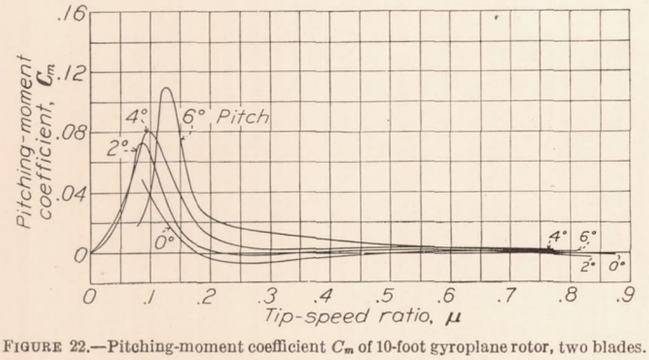

FIGURE 22.—Pitching-moment coefficient C_m of 10-foot gyroplane rotor, two blades.

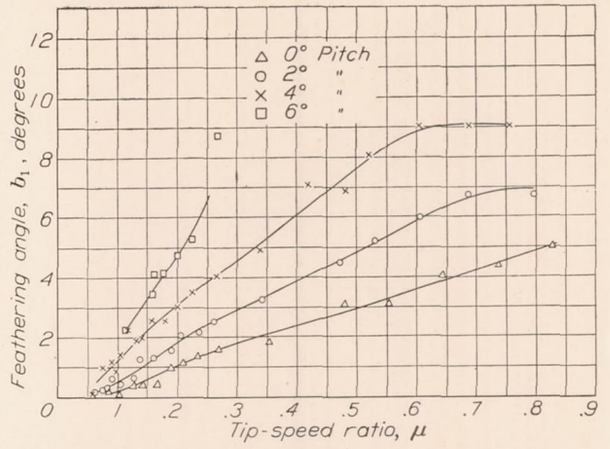

FIGURE 19.—Feathering angle b_1 for zero rolling moment, 10-foot gyroplane rotor two blades.

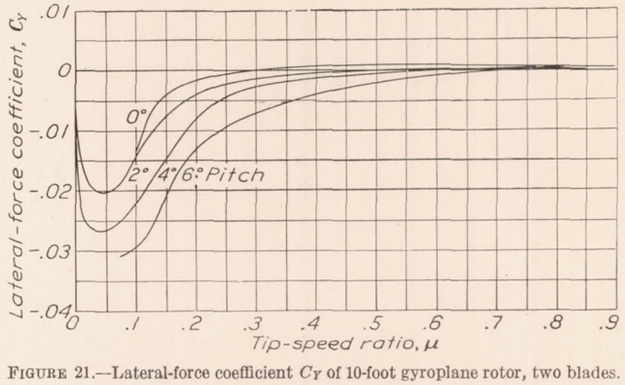

FIGURE 21.—Lateral-force coefficient C_Y of 10-foot gyroplane rotor, two blades.

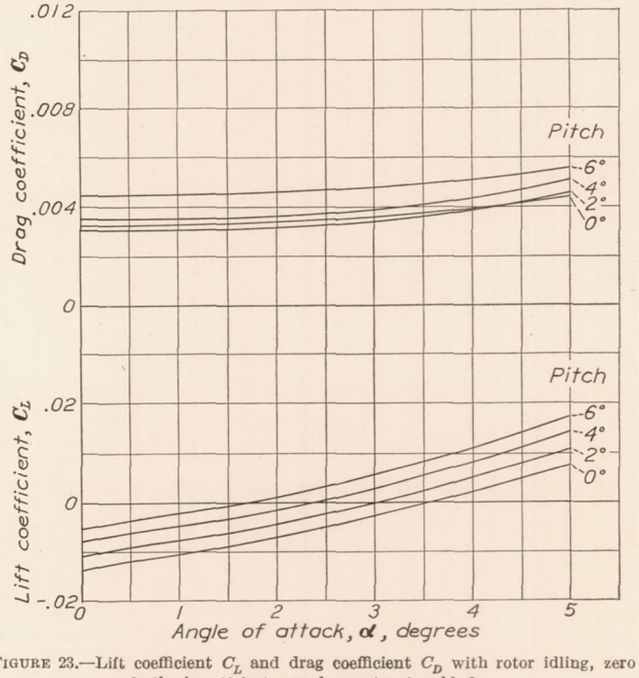

FIGURE 23.—Lift coefficient C_L and drag coefficient C_D with rotor idling, zero feathering, 10-foot gyroplane rotor, two blades.

Angle of attack.—Figures 8 and 18 show the angles of attack for each pitch setting tested as functions of the tip-speed ratio. At low tip-speed ratios the angle of attack at a given μ varies consistently with the pitch setting, but the variation becomes irregular as the tip-speed ratio increases. This illogical behavior of the angle of attack is probably caused by the fact that the dispersion of the test results at high tip-speed ratios was very large and also by the condition that the average rolling moment was not zero in that range and was different at different pitch settings. The angle of attack is useful primarily in the application of the equations in reference 1 to the transformation of the test results to a different solidity; it is not a fundamental variable, although it helps to determine the tip-speed ratio.

Idling tests.—It has been proposed that the gyroplane rotor be used in combination with a fixed wing so that at high speed the angle of attack of the rotor can be decreased until it rotates very slowly, and the machine can then be supported solely by the fixed wing. In order to determine whether the efficiency of the machine would thereby be increased, the lift and drag of the idling rotor with zero feathering angle were determined and are shown in figures 13 and 23. Because of the existing uncertainty regarding the tare drag, the absolute value of the drag of the idling rotor is unreliable but the influence of pitch setting is clearly shown. As was expected, the lift and drag coefficients increased with pitch setting except at low pitch settings on the two-bladed rotor. The discrepancy is considered to be accidental because of the difficulty encountered in measuring such small forces.

Solidity.—The influence of a change in the rotor solidity can be ascertained by a comparison of the results obtained on the four-bladed rotor (figs. 4 to 13) with those obtained on the two-bladed rotor (figs. 14 to 23). The thrust coefficient is shown to be directly proportional to the solidity, as is the lift coefficient at high tip-speed ratios. At lower tip-speed ratios and high angles of attack, the lift coefficient is not proportional to the solidity because of a simultaneous change in the angle of attack at a given tip-speed ratio. Thus, the maximum lift coefficient of the four-bladed rotor at 5° pitch setting was 0.9; whereas for the two-bladed rotor it was 0.8.

The influence of solidity on the L/D as shown in figures 5 and 15 is not considered to be reliable because the tare drag is not accurately known. A change in the tare drag would alter the relative positions of the four-bladed and two-bladed L/D curves and would conceivably reverse them to indicate that the two-bladed rotor was the more efficient.

Application of results.—The test results are considered to be important in that they establish the influence of pitch setting and solidity upon most of the rotor characteristics and constitute the first published information on the control moments obtainable with the feathering control. The test shows the promise inherent in the gyroplane rotor and justifies further experimentation to the end of removing some of the uncertainties in this work as well as improving the characteristics obtained.

The quantitative application of the results in this paper can be justified for all characteristics except the lift-drag ratio. In work of this kind the determination of the proper tare drag is extremely difficult, and the results must be interpreted with that fact in mind. Some errors may arise because of the difference in scale between the model and the full-scale rotors, but it is thought that such effects will not be serious.

CONCLUSIONS

1. These model tests, because of the excessive size of the rotor hub, are unreliable as regards the lift-drag ratio of a gyroplane rotor.
2. The pitch setting is the critical parameter that determines rotor characteristics.
3. A change in solidity causes a proportional change in rotor-force coefficients only at high tip-speed ratios.
4. The rate of change of rolling moment with feathering angle is not materially influenced by pitch angle or solidity and decreases dangerously at low tip-speed ratios.
5. The maximum resultant force coefficient is obtained with a pitch setting of 5°.
6. A feathering angle considerably greater than 10° is required to obtain zero rolling moment at high tip-speed ratios for pitch settings greater than 4°.

LANGLEY MEMORIAL AERONAUTICAL LABORATORY,
NATIONAL ADVISORY COMMITTEE FOR AERONAUTICS,
LANGLEY FIELD, VA., *April 11, 1935.*

REFERENCES

1. Wheatley, John B.: The Aerodynamic Analysis of the Gyroplane Rotating-Wing System. T. N. No. 492, N. A. C. A., 1934.
2. Weick, Fred E., and Wood, Donald H.: The Twenty-Foot Propeller Research Tunnel of the National Advisory Committee for Aeronautics. T. R. No. 300, N. A. C. A., 1928.

U. S. GOVERNMENT PRINTING OFFICE: 1935

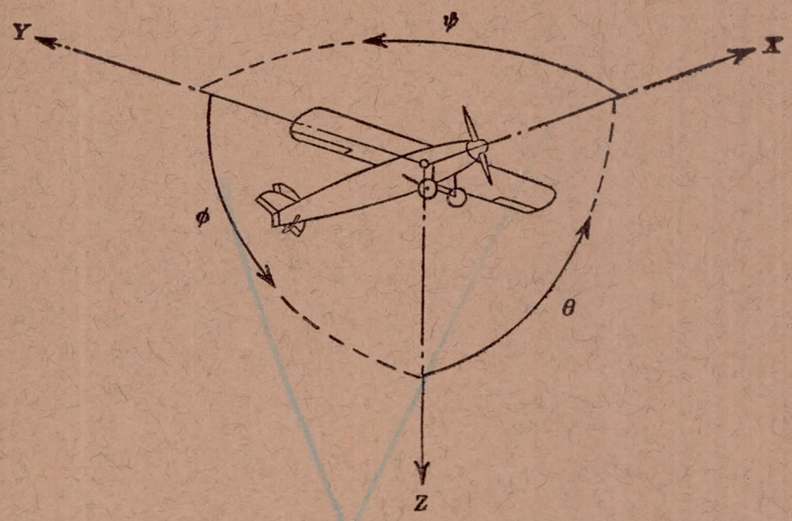

Positive directions of axes and angles (forces and moments) are shown by arrows

Axis		Force (parallel to axis) symbol	Moment about axis			Angle		Velocities	
Designation	Symbol		Designation	Symbol	Positive direction	Designation	Symbol	Linear (component along axis)	Angular
Longitudinal	X	X	Rolling	L	$Y \longrightarrow Z$	Roll	ϕ	u	p
Lateral	Y	Y	Pitching	M	$Z \longrightarrow X$	Pitch	θ	v	q
Normal	Z	Z	Yawing	N	$X \longrightarrow Y$	Yaw	ψ	w	r

Absolute coefficients of moment

$C_l = \frac{L}{qb\bar{S}}$ (rolling) $\quad C_m = \frac{M}{qc\bar{S}}$ (pitching) $\quad C_n = \frac{N}{qb\bar{S}}$ (yawing)

Angle of set of control surface (relative to neutral position), δ. (Indicate surface by proper subscript.)

4. PROPELLER SYMBOLS

D, Diameter

p, Geometric pitch

p/D, Pitch ratio

V', Inflow velocity

V_s, Slipstream velocity

T, Thrust, absolute coefficient $C_T = \frac{T}{\rho n^2 D^4}$

Q, Torque, absolute coefficient $C_Q = \frac{Q}{\rho n^2 D^5}$

P, Power, absolute coefficient $C_P = \frac{P}{\rho n^3 D^5}$

C_s, Speed-power coefficient $= \sqrt[5]{\frac{\rho V^5}{P n^2}}$

η, Efficiency

n, Revolutions per second, r.p.s.

Φ, Effective helix angle $= \tan^{-1}\left(\frac{V}{2\pi r n}\right)$

5. NUMERICAL RELATIONS

1 hp. = 76.04 kg-m/s = 550 ft-lb./sec.
1 metric horsepower = 1.0132 hp.
1 m.p.h. = 0.4470 m.p.s.
1 m.p.s. = 2.2369 m.p.h

1 lb. = 0.4536 kg.
1 kg = 2.2046 lb.
1 mi. = 1,609.35 m = 5,280 ft.
1 m = 3.2808 ft.